The Cooper Pair Pump as a Quantized Current Source

Raphaël Leone, Laurent Lévy, Philippe Lafarge

The Cooper Pair Pump as a Quantized Current Source

R. Leone and L. P. Lévy
Institut Néel, C.N.R.S.- Université Joseph Fourier, BP 166, 38042 Grenoble Cedex 9, France

P. Lafarge
Laboratoire Matériaux et Phénomènes Quantiques, Université Paris Diderot - Paris 7, C.N.R.S. UMR 7162, 75205 Paris Cedex 13, France

(Dated: November 1, 2007)

A new charge quantization in a phase-polarized Cooper Pair Pump (CPP) is proposed, based on the topological properties of its Hamiltonian ground state over a three-dimensional parameter space $\mathbb{P}$. The charge is quantized using a set of path in $\mathbb{P}$ covering the surface of a torus, and is a multiple of the integer Chern index c_1 of this surface. This quantization is asymptotic but the pumped charge converges rapidly to the quantized value with the increase in the path frequency. The topological nature of the current makes this CPP implementation an excellent candidate for a metrological current standard.

PACS numbers: 85.25.Cp, 03.65.Vf, 74.50.+r, 74.78.Na

Topological defects occur in a number of different settings. In superfluids or magnets, the ground state is described by an order parameter. Topological defects (vortices, skyrmions...) are singular points of the order parameter field[1]. A topological charge is assigned to the mapping from physical space to order parameter space. In quantum systems with few degrees of freedom, the energy levels and eigenstates may depend on a set of continuous classical parameters (or band indices). When the number of parameters is sufficient (three for a complex Hamiltonian), isolated degeneracies between two neighboring levels (or bands) can occur. The presence of a degeneracy has many physical consequences. For quantum wavefunctions, the degeneracies can then be viewed as a defect in their phase field[2]. Some classical examples are well known in polyatomic molecules[3], where the nuclear coordinates form a set of semiclassical parameters (within the Born-Oppenheimer approximation) for the electronic structure. Energy manifolds can have conical intersections at isolated values of the nuclear coordinates[4, 5]. When a topological charge is assigned to these degeneracies, the change of multiplicity of rotation-vibrations levels as a function of nuclear coordinates are easily understood in topological terms. In molecular magnets, isolated degeneracies have also been found for specific directions and values of the magnetic field[6, 7]. The integer quantum Hall effect has also been interpreted in term of Chern indices[8, 9] which are the total topological charge included within a filled Landau band. In all these examples, a topological charge is associated to an isolated degeneracy between neighboring bands, where the defect in the wavefunctions phase field occur. Its physics can be described by a "monopole" placed at the degenerate point in parameter space. The flux of the magnetic field produced by the monopole through any surface enclosing the defect is proportional to the Chern index for this surface. For a the two dimensional electron gas, the Hall conductivity of a band is $\sigma_{xy} = \frac{e^2}{h} \times c_1$ where c_1 is the Chern index assigned to the band[8]. The phase change of a wavefunction on a closed path is proportional to the integral of the potential vector, which is also the flux through the surface bounded by the path. This phase change, better known as Berry's phase, takes a particular value (π) for some of the physically relevant paths enclosing degeneracies. In molecular magnets, this phase change leads to destructive interferences which quench quantum tunnelling at the degeneracy points.

In this letter, the relevance of this physics to superconducting circuits is illustrated around an example, the Cooper Pair Pump (CPP), which lowest two energy levels form two bands which depend on continuous parameters (gate charges or voltages and magnetic flux). The parameter space is in this case three dimensional and degeneracies (defects) occur at isolated points in parameter space. We demonstrate how a charge quantization, proportional to the defect topological charge, can be exploited to produce a current source with metrological accuracy.

The CPP-circuit represented in Fig. 1 includes a small inductance in serie with the Cooper pair pump. The CPP has three Josephson junctions in series which define two superconducting islands. As long as the device is dominated by the Coulomb charging energy $E_C = \frac{(2e)^2}{4C}$ of the islands, the topological properties of the circuit do not

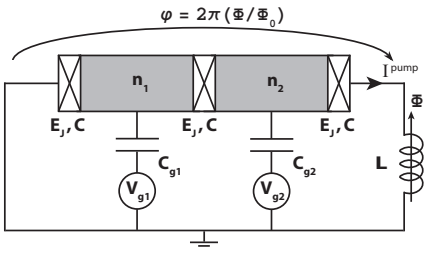

FIG. 1: The Cooper Pair Pump.

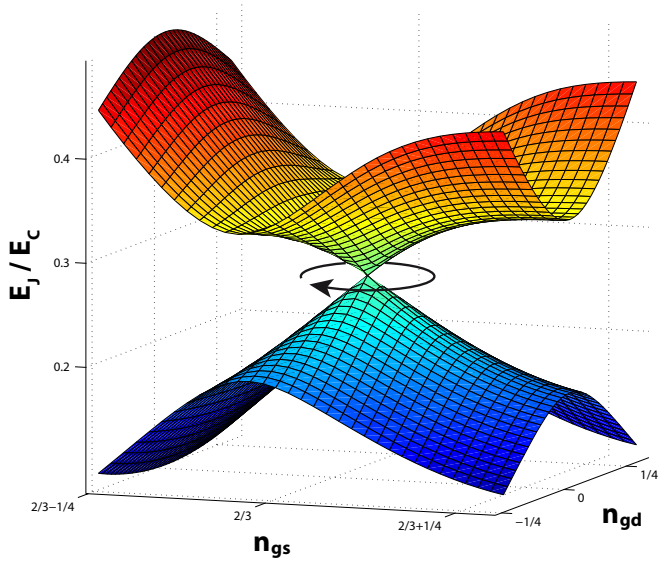

FIG. 2: (Color) Plot of the energies (in units of the charging energy) of the two lowest levels as a function of the gate charges n_{gs} and n_{gd} at $\varphi = \pi$ in the vicinity of the vertex $\mathbf{T_1}$. This "diabolical point" is a conical intersection of the energy sheets between the two lowest bands. It represents a topological defect in the wavefunction phase fields and cannot be removed by any perturbations which merely shift its position in parameter space.

depend on the precise value of the Josephson couplings E_J or capacitances C, which can be taken as identical. Let n_1 and n_2 be the number of Cooper pairs in excess on each island and $n_{g1} = \frac{C_{g1}V_{g1}}{2e}$, $n_{g2} = \frac{C_{g2}V_{g2}}{2e}$, the polarization charge induced by two gate voltages V_{g1} and V_{g2}. The electrostatic charges on each island are $n_1 - n_{g1}$ and $n_2 - n_{g2}$, where n_{g1} and n_{g2} are classical variables tuning the islands electrostatic energies. The inductance L serves two purposes: the phase $\hat{\phi}$ across the CPP is controlled by the magnetic flux Φ it threads, and it is also used as the input for the readout circuit measuring the circulating current through the pump. For a small inductance, the magnetic energy $\frac{1}{2L}\left(\hat{\phi} - 2\pi\frac{\Phi}{\Phi_0}\right)^2$ defines a sufficiently deep potential minimum: quantum fluctuations of $\hat{\phi}$ across the CPP are quenched and the phase bias is set by the "classical" phase $\varphi = 2\pi\frac{\Phi}{\Phi_0}$. The circuit energy can be tuned through three independent parameters n_{g1}, n_{g2} and φ defining the parameter space $\mathbb{P}$.

Charging $\mathcal{H}_C$ and Josephson $\mathcal{H}_J$ Hamiltonian contribute to the CPP energy. It is convenient to write the charging energy in term of $\hat{n}_s = \hat{n}_1 + \hat{n}_2$, the total charge on the CPP and $\hat{n}_d = \hat{n}_1 - \hat{n}_2$, the charge imbalance between the two islands. Their canonical conjugates, the phase variables $\hat{\Theta}_s$ and $\hat{\Theta}_d$ enter in the Josephson Hamiltonian. In term of $\hat{n}_s$ and $\hat{n}_d$ the charging Hamiltonian is

$$\mathcal{H}_C = E_C\left[\left(\hat{n}_s - n_{gs}\right)^2 + \kappa_0\left(\hat{n}_d - n_{gd}\right)^2\right], \qquad (1)$$

where $E_C = \frac{(2e)^2}{4C}$, $n_{gs} = n_{g1} + n_{g2}$, $n_{gd} = n_{g1} - n_{g2}$ are the corresponding polarization charges and $\kappa_0 = \frac{1}{3}$ is a capacitance ratio. Each eigenstate $|n_s, n_d\rangle$ is the ground state of $\mathcal{H}_C$ inside an hexagonal area $h_{(n_s,n_d)}$, centered at the point (n_{gs}= n_s, n_{gd}= n_d), in the n_{gs}-n_{gd} plane (shown as the base plane in Fig. 3). Its boundaries are electrostatic degeneracy lines between "neighboring" charge states, and the vertices are points of triple degeneracies. The vertices $\{T_1\} = (n_{gs} = \frac{2}{3}, n_{gd} = 0)$ and $\{T_2\} = (n_{gs} = \frac{4}{3}, n_{gd} = 0)$ form the unit cell of this hexagonal lattice. With an appropriate gauge choice, the Josephson Hamiltonian $\mathcal{H}_J$ depends on the phase bias φ as

$$\mathcal{H}_J = -2E_J \cos\hat{\Theta}_s \cos\hat{\Theta}_d - E_J \cos(2\hat{\Theta}_d + \varphi)\,. \qquad (2)$$

The total Hamiltonian is 2π-periodic in φ. Lattice translations in the hexagonal lattice (n_{gs}-n_{gd}) connect equivalent but physically different states. Because the parameter space $\mathbb{P}$ is three dimensional, $\mathcal{H}_J$ lifts the electrostatic degeneracies except at *isolated points* where the ground level is still degenerate, in $\mathbb{P}$ (a consequence of the von Neumann-Wigner theorem[10]). These points occur at the vertices $\{T_1\}$ and $\{T_2\}$ of the hexagonal lattice for $\varphi = \pi$, as illustrated in Fig. 2. In realistic implementation of the Cooper pair pump, it is favorable to keep the ratio between Josephson and charging energy $\beta = \frac{E_J}{E_C}$ small, an assumption made throughout this paper.

In the limit of zero Josephson coupling, the electrostatic states $|0,0\rangle, |1,1\rangle$ and $|1,-1\rangle$ are degenerate at the vertex $\{T_1\}$. For finite Josephson couplings, the ground state remains degenerate at this point when $\varphi = \pi$. The two degenerate ground states at $\mathbf{T_1} = \{T_1, \pi\}$ are

$$|g_\pm\rangle = \frac{1}{\sqrt{3}}\left[|0,0\rangle \mp \frac{\sqrt{3}\mp 1}{2}|1,1\rangle \pm \frac{\sqrt{3}\pm 1}{2}|1,-1\rangle\right] \qquad (3)$$

with energy $E_g(\mathbf{T_1}) = \frac{4}{9}E_C - \frac{1}{2}E_J$ while the first excited state $|e\rangle$ is well separated from the ground state ($E_e = E_g + \frac{3E_J}{2}$). For a small deviation $\delta\mathbf{R} = \left(\sigma = n_{gs} - \frac{2}{3}, \delta = n_{gd}, \psi = \varphi - \pi\right)$ from degeneracy $\mathbf{T_1}$, a two-level approximation ($|g_\pm\rangle$) is appropriate for small β. The eigenenergies $E_\pm(\delta\mathbf{R}) = E_g \pm \frac{2}{3}E_C\sqrt{\sigma^2 + \frac{\delta^2}{3} + \frac{3}{16}\beta^2\psi^2}$ display a characteristic conical intersection at $\mathbf{T_1}$. After rescaling the deviation $\delta\mathbf{R}$ from $\mathbf{T_1}$, as $b_x = \frac{4}{3}E_C\,\sigma, b_y = -\frac{1}{\sqrt{3}}E_J\,\psi, b_z = \frac{4}{4\sqrt{3}}\,\delta$, the two-level Hamiltonian maps onto an isotropic spin-$\frac{1}{2}$ problem,

$$\hat{\mathcal{H}}_{\pm(\mathbf{T_1})}(\mathbf{R}) = E_g\mathbf{1} + \frac{1}{2}\boldsymbol{\sigma}\cdot\mathbf{b}(\mathbf{R}). \qquad (4)$$

This makes the conical nature of the intersection explicit ($E_\pm(\delta\mathbf{R}) = E_g \pm \frac{|\mathbf{b}|}{2}$), and spinor eigenstates can be specified using the direction of $\mathbf{b}$ rather than $\delta\mathbf{R}$.

The topological nature of this degeneracy becomes clear when considering the adiabatic evolution of quantum states along different closed paths Γ "around" this

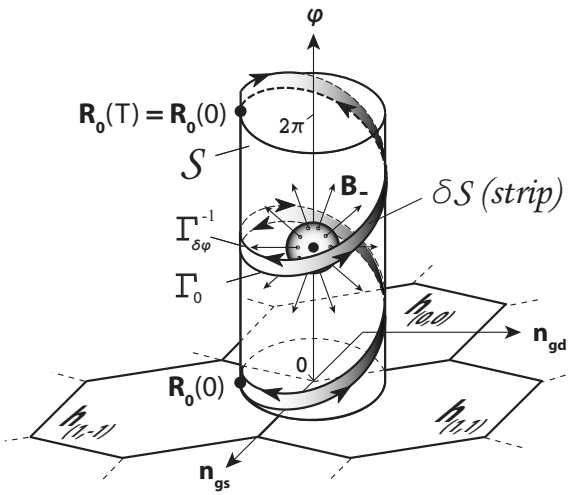

FIG. 3: Representation of the degeneracy point $\{T_1, \varphi = \pi\}$ in the parameter space $\mathbb{P}$. The cylindrical surface which encloses this point has the topology of a torus. The Chern index is defined as the flux through this surface normalized by 2π. Several paths on this cylinder are considered in the text.

point. One of them is represented in Fig. 3 as the time evolution of a point $\mathbf{R}(t)$ in $\mathbb{P}$. If $|g_\pm(\mathbf{R}(t))\rangle$ are instantaneous eigenstates of the Hamiltonian, after a period T around any closed path $|g_\pm(T)\rangle = e^{-i(\eta_\pm - \gamma_\pm)}|g_\pm(0)\rangle$ depends on two phases, $\eta_\pm = \frac{1}{\hbar}\int_0^T E_{g_\pm}(\mathbf{R}(t))dt$, the dynamical phase and $\gamma_\pm = i\oint_\Gamma \mathbf{A}_\pm(\mathbf{R})\cdot d\mathbf{R}$, the geometrical phase. It is expressed as an integral of the vector potential $\mathbf{A}_\pm(\mathbf{R}) = \langle g_\pm(\mathbf{R})|\boldsymbol{\nabla} g_\pm(\mathbf{R})\rangle$ over the path. If the closed paths considered are sufficiently close to the degeneracy $\mathbf{T_1}$ where the two-level approximation is valid, Berry's geometrical phase can also be computed using the spin-$\frac{1}{2}$ representation as $\gamma_\pm = i\oint_\Gamma \mathbf{A}_\pm(\mathbf{b})\cdot d\mathbf{b}$, where the vector potential is azimuthal in this textbook example: $\mathbf{A}_\pm(\mathbf{b}) = \pm\frac{\cos\theta\mp 1}{2|\mathbf{b}|\sin\theta}\,\mathbf{e}_\phi$ (the Euler angles θ, ϕ specify the direction of $\mathbf{b}$). Its line integral over a closed path Γ is $\gamma_\pm(\Gamma) = \mp\frac{\Omega(\Gamma)}{2}$, where $\Omega(\Gamma)$ is the solid angle seen from the degeneracy. The vector potentials $\mathbf{A}_\pm(\mathbf{b})$ can be recognized as the gauge field of Dirac monopoles of strength $\mp\frac{1}{2}$ placed at $\mathbf{T_1}$. They produce a radial magnetic field $\mathbf{B}_\pm = \mp\frac{\mathbf{b}}{2|\mathbf{b}|^3}$ which flux is $\mp 2\pi$ when integrated over any surface enclosing this single degeneracy. When normalized to 2π, this flux gives the Chern index $c_1^{(\pm)} = \mp 1$ of the surface with respect to the eigenstates $|g_\pm\rangle$ and one assignes to the degeneracy $\mathbf{T_1}$ topological charges $q_\pm(\mathbf{T_1}) = \mp 1$.

This topological picture is not restricted to the immediate neighborhood of $\mathbf{T_1}$ where a two-level approximation can be made. Let us consider the cylindrical surface represented in Fig. 3. Since the top and bottom planes $\varphi = 0$ and $\varphi = 2\pi$ are physically equivalent, this cylinder has the topology of a torus, and its surface is the constant radius $|\mathbf{R}| = \rho$ cylinder. The magnetic flux of $\mathbf{B}_- = \boldsymbol{\nabla}\times\mathbf{A}_-$ through this closed surface *defines* its Chern index $c_1^{(-)}$ of the ground state $|g_-(\mathbf{R})\rangle$[11]. This index is non-zero only if the topology is non trivial, i.e. if the surface encloses degeneracies. Here the "cylindrical surface" encloses only the isolated degeneracy $\mathbf{T_1}$ and Gauss theorem guarantees that its index is identical to the one of the small sphere around $\mathbf{T_1}$ just considered. For a cylinder around $\mathbf{T_2} = \{T_2, \pi\}$ the Chern indices have opposite sign and $q_\pm(\mathbf{T_2}) = \pm 1$. For a larger surface, the Chern index is the sum of the topological charges it encloses and when no degeneracies are present, it is zero.

In a CPP, pumping of charges through the circuit is achieved when moving the ground state $|g_-(\mathbf{R})\rangle$ adiabatically along a one-dimensional path in $\mathbb{P}$. In the literature, the paths considered so far have been closed trajectories around $\{T_1\}$ or $\{T_2\}$ at constant φ for which the charge transferred is not quantized. *When the path is chosen to cover a surface enclosing one of the singularities, the charge transferred becomes an integer multiple of the ground state Chern index.* This quantization is not only observable but can be exploited to make a current standard of metrological accuracy, in a similar way as the quantum Hall effect is a standard of resistance based on the Chern indices of Landau bands. Let us consider a helical path Γ_{φ_0} on the surface of the cylinder (Fig. 3) starting from the plane $\varphi = \varphi_0$ and ending in the plane $\varphi = \varphi_0 + 2\pi$ while making an integer number p of windings (in Fig. 3, $\varphi_0 = 0$ and $p = 2$). The pumped charge $Q^{\rm pump}$ on this path has a dynamical $Q^{\rm dyn}$ and a geometrical contribution $Q^{\rm geo}$. The expressions

$$Q^{\rm dyn} = 2e\frac{d\eta_-}{d\varphi_0}(\Gamma_{\varphi_0}), \quad Q^{\rm geo} = -2e\frac{d\gamma_-}{d\varphi_0}(\Gamma_{\varphi_0}), \qquad (5)$$

proved elsewere[12], generalize earlier results[13, 14] to arbitrary three dimensional closed paths in $\mathbb{P}$. We first show that the geometrical contribution is quantized when averaged over the initial phase φ_0 of the helix. Taking two helices Γ_{φ_0} and $\Gamma_{\varphi_0+\delta\varphi}$ shifted in φ by an infinitesimal increment $\delta\varphi$, a closed path $\Sigma(\varphi_0)$ on the surface of the cylinder (shown in Fig. 3) can be constructed by adding two small opposite "vertical" segments connecting the paths Γ_{φ_0} and $\Gamma^{-1}_{\varphi_0+\delta\varphi}$ which line integrals cancel. Using Eq. 5, the transferred charge is

$$Q^{\rm geo} = 2e\frac{\gamma_-(\Gamma_{\varphi_0}) + \gamma_-(\Gamma^{-1}_{\varphi_0+\delta\varphi})}{\delta\varphi} = 2e\frac{\gamma_-\big(\Sigma(\varphi_0)\big)}{\delta\varphi}\,. \quad (6)$$

Using Stokes theorem, the above numerator is also $\iint_{\delta\mathcal{S}} \mathbf{B}_-(\mathbf{R})\cdot\hat{n}\,dS$, where $\delta\mathcal{S}$ is the surface of the strip between the two helices (shown in Fig. 3 for $\varphi_0 = 0$) and $\mathbf{B}_-(\mathbf{R})$ is the "magnetic" field produced by the monopole at the degeneracy. When the initial angle φ_0 is integrated from 0 to 2π, adding all the elementary strips $\delta\mathcal{S}$ gener-

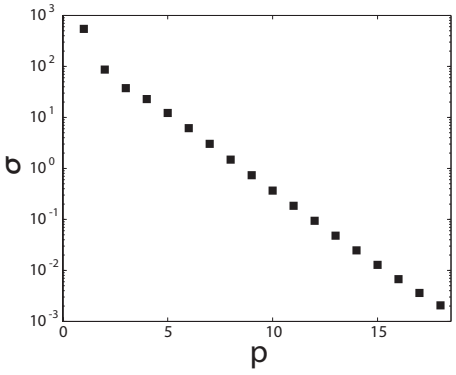

FIG. 4: Plot of the peak amplitude of $Q^{\rm dyn}(\Gamma_{\varphi_0})$ as a function of the number of windings p in the interval $[\varphi_0;\varphi_0+2\pi]$ for a charging energy of 10 meV, a Josephson coupling $E_J=0.5E_C$ and a period of 10^{-6} sec.

ates p times the total surface $\mathcal{S}$ (Fig. 3). Hence

$$\langle Q^{\rm geo}\rangle_{\varphi_0}=\frac{2e}{2\pi}\oiint_{\mathcal{S}}\mathbf{B}_-\cdot\hat{n}\,dS=2e\,p\,c_1^{(-)}(\mathcal{S})=2e\,p \quad (7)$$

is quantized by the Chern index c_1 of the cylindrical surface $\mathcal{S}$ (torus). It is not necessary to average over φ_0 to reach quantization. If the number of windings p in Γ is large, the path integral of $\mathbf{A}_-$ over Γ reaches the surface integral of $\mathbf{B}_-$ over the cylinder and $Q^{\rm geo}\overset{p\to\infty}{=}2e\,p$. The increase of accuracy with p being roughly an order of magnitude per additional winding, this is not only practical but also quite accurate. Using the same procedures, the dynamical charge $Q^{\rm dyn}$ averages out to zero because $\eta_-(\Gamma_{\varphi_0})$ is a 2π-periodic function of φ_0 since the Hamiltonian is 2π-periodic in φ. Its magnitude $\simeq\frac{T}{\hbar}\frac{E_J^3}{E_C^2}$ depends critically on the ratio $\beta=\frac{E_J}{E_C}$, however the periodic and odd-dependence of $Q_{\rm dyn}$ with φ_0 guarantees that its φ_0-average is zero. In realistic situations, φ_0 may not be completely controlled, or the path may not close perfectly because of flux-noise. It is therefore instructive to plot the evolution of the peak amplitude of $Q^{\rm dyn}$ as a function of the number of winding p in a $\varphi-$period. In Fig. 4, this peak amplitude looses four order of magnitudes when p is increased by 10, using a ratio $\beta=0.5$ an order of magnitude larger than its optimal value. For smaller β, the decrease is even more dramatic. Hence, the CPP delivers a very accurate DC current

$$I^{\rm pump}=Q^{\rm pump}\,\nu\overset{p\to\infty}{=}2e\,\nu\,, \quad (8)$$

where ν is the winding frequency.

We now consider the possible sources of errors in a practical implementation of this circuit as a current standard. Low frequency noise in the parameters will introduce some jitter in the path covered in $\mathbb{P}$: the surface generated by the path will not be a perfect cylinder. On the other hand, as long as the jitter amplitude is small compared to the radius, the surface generated still encloses the topological charge, and no significant error in quantization should result. The most detrimental source of error comes from inelastic transitions between the ground state and the first excited state in the adiabatic evolution, because their topological charges are opposite. This means that if the time spent in the first exited state is τ in a period, the relative error in the transferred charge will be $-4e\frac{\tau}{T}$. There are two ways this can happen. For each winding around T_1, three saddle points between the ground and first excited manifolds have to be crossed (along the hexagonal lines shown in Fig. 3), where the probability of Landau-Zener tunnelling is largest. For the optimal radius ($\simeq\frac{1}{3}$) this tunnelling probability is of order $P\simeq e^{-\left(\frac{3\pi}{2}\right)^2\frac{E_J}{E_C}\frac{E_J}{h\nu}}$. To stay below the part per million level requires that the winding frequency ν to stay below 100 MHz for a Josephson coupling of $0.05E_C$, limiting the pumped current amplitude $2e\nu$ to 32 pA. The other source of inelastic transitions to the first excited state is the back-action of the measuring device on the CPP, which needs to be rigourously controlled.

The physics discussed in this paper is by no means limited to the CPP: as long as a circuit has three tunable parameters or more, degeneracies can occur. In this paper, we emphasized the topological quantization and its strong robustness to adiabatic parameters fluctuations, a key point for metrological applications. The realization of this metrological source is under way in our group: it is a beautiful scientific challenge for fundamental quantum electronics of real practical value. R. Leone is supported by a fellowship of the Rhône-Alpes Micro-Nano cluster. The authors are grateful to F. Faure for enlightening discussions.

[1] N. D. Mermin, Rev. Mod. Phys. **51**, 591 (1979).
[2] M. V. Berry, Proc. R. Soc. Lond. A **392**, 45 (1984).
[3] G. Herzberg and H. C. Longuet-Higgins, Disc. Faraday Soc. **35**, 77 (1963).
[4] F. Faure and B. Zhilinskii, Phys. Rev. Lett. **85**, 960 (2000).
[5] B. I. Zhilinskii, Phys. Rep. **341**, 85 (2001).
[6] W. Wernsdorfer and R. Sessoli, Science, **284**, 133 (1999); W. Wernsdorfer, N. E. Chakov and G. Christou, Phys. Rev. Lett. **95**, 037203 (2005).
[7] P. Bruno, Phys. Rev. Lett. **96**, 117208 (2006).
[8] D. J. Thouless, M. Kohmoto, P. Nightingale and M. den Nijs, Phys. Rev. Lett. **49**, 405 (1982); D. J. Thouless, Phys. Rev. B **27**, 6083 (1983).
[9] M. Kohmoto, Ann. of Phys. **160**, 296 (1984).
[10] J. von Neumann and E. P. Wigner, Phys. Zschr. **30**, 467 (1929).
[11] B. Simon, Phys. Rev. Lett. **51**, 2167 (1983).
[12] R. Leone and L. P. Lévy, (unpublished).
[13] M. Aunola and J. J. Toppari, Phys. Rev. B **68**, 020502(R) (2003).
[14] M. Möttönen, J. P. Pekola, J. J. Vartinainen, V. Brosco, F. Hekking, Phys. Rev. B **73**, 214523 (2006).